

Seasonal variation in denitrification and dissimilatory nitrate reduction to ammonia process rates and corresponding key functional genes along an estuarine nitrate gradient

Cindy J Smith, Liang F Dong, John Wilson, Andrew Stott, Andrew Mark Osborn and David B Nedwell

Journal Name: Frontiers in Microbiology
ISSN: 1664-302X
Article type: Original Research Article
Received on: 20 Mar 2015
Accepted on: 17 May 2015
Provisional PDF published on: 17 May 2015
Frontiers website link: www.frontiersin.org
Citation: Smith CJ, Dong LF, Wilson J, Stott A, Osborn AM and Nedwell DB(2015) Seasonal variation in denitrification and dissimilatory nitrate reduction to ammonia process rates and corresponding key functional genes along an estuarine nitrate gradient. *Front. Microbiol.* 6:542. doi:10.3389/fmicb.2015.00542
Copyright statement: © 2015 Smith, Dong, Wilson, Stott, Osborn and Nedwell. This is an open-access article distributed under the terms of the [Creative Commons Attribution License \(CC BY\)](http://creativecommons.org/licenses/by/2.0/). The use, distribution and reproduction in other forums is permitted, provided the original author(s) or licensor are credited and that the original publication in this journal is cited, in accordance with accepted academic practice. No use, distribution or reproduction is permitted which does not comply with these terms.

This Provisional PDF corresponds to the article as it appeared upon acceptance, after rigorous peer-review. Fully formatted PDF and full text (HTML) versions will be made available soon.

1 **Seasonal variation in denitrification and dissimilatory nitrate reduction to**
2 **ammonia process rates and corresponding key functional genes along an**
3 **estuarine nitrate gradient.**

4
5 Cindy J. Smith^{1,2,‡^{a*}}, Liang. F. Dong^{1,‡}, John Wilson², Andrew Stott³, A. Mark Osborn^{2b} and
6 David B. Nedwell¹

7 ¹ Department of Biological Sciences, University of Essex, Wivenhoe Park, Colchester CO4
8 3SQ U.K.

9 ² Department of Animal and Plant Sciences, The University of Sheffield, Western Bank,
10 Sheffield S10 2TN U.K.

11 ³ NERC Life Sciences Mass Spectrometer Facility, Centre for Ecology & Hydrology,
12 Lancaster Environment Centre, Lancaster LA1 4AP U.K.

13 ^a Present address: Microbiology, School of Natural Sciences, NUI Galway, University Road,
14 Galway, Ireland.

15 ^b Present address: School of Applied Sciences, RMIT University, Bundoora VIC 3083,
16 Australia. PO Box 77

17
18 ‡ C.J.S and L.F.D contributed equally to this research

19 * Corresponding author

20 Tel. 353 91 493832

21 Fax 353 91 494598

22 Email cindy.smith@nuigalway.ie

23 **Running title:** Seasonal variation in estuarine nitrate-reduction

24 **Keywords:** Denitrification / DNRA / *narG*, *napA*, *nirS*, *nrfA* / (RT)-Q-PCR

25

26 **ABSTRACT**

27 This research investigated spatial-temporal variation in benthic bacterial community structure,
28 rates of denitrification and dissimilatory nitrate reduction to ammonium (DNRA) processes
29 and abundances of corresponding genes and transcripts at three sites – the estuary-head, mid-
30 estuary and the estuary mouth along the nitrate gradient of the Colne estuary over an annual
31 cycle. Denitrification rates declined down the estuary, while DNRA rates were higher at the
32 estuary head and middle than the estuary mouth. In four out of the six two-monthly time-
33 points, rates of DNRA were greater than denitrification at each site. Abundance of gene
34 markers for nitrate-reduction (nitrate reductase *narG* and *napA*), denitrification (nitrite
35 reductase *nirS*) and DNRA (DNRA nitrite reductase *nrfA*) declined along the estuary with
36 significant relationships between denitrification and *nirS* abundance, and DNRA and *nrfA*
37 abundance. Spatially, rates of denitrification, DNRA and corresponding functional gene
38 abundances decreased along the estuary. However, temporal correlations between rate
39 processes and functional gene and transcript abundances were not observed.

40

41 **INTRODUCTION**

42 Estuarine sediments are natural environmental gradients of nutrients and salinity, and
43 significant sites of microbial diversity and activity. Bacterial diversity within these sediments
44 is often higher than in other environments (Lozupone and Knight 2007) and the bacteria
45 present drive essential nutrient cycles with direct consequences for ecosystem function.
46 Previously, we showed that the largest nutrient loads to all mainland UK estuaries were
47 attributable to nitrate: at least an order of magnitude greater than ammonium (Nedwell *et al.*,
48 2002; Earl *et al.*, 2014). Benthic microorganisms mediate the nitrate load entering coastal
49 waters via denitrification, dissimilatory nitrate reduction to ammonia (DNRA) and anaerobic
50 ammonia oxidation (anammox) processes.

51 Heterotrophic denitrification by facultatively anaerobic bacteria using nitrate to respire
52 organic matter, produces N_2 and to a lesser extent the greenhouse gas N_2O (Seitzinger *et*
53 *al.*, 1988; Nedwell *et al.*, 1999; Dong *et al.*, 2002), removing up to 50% of the nitrate load
54 from estuaries (Nedwell *et al.*, 1999). Anammox, the anaerobic autotrophic oxidization of
55 NH_4^+ , uses NO_2^- as an electron acceptor yielding N_2 , (Strous *et al.*, 1999; Kuenen 2008).
56 Reported values of N_2 production from anammox in estuarine sediments range from 0 to 30%
57 (Brin *et al.*, 2014, Dong *et al.*, 2009, Nicholls and Trimmer 2009). Denitrification and
58 anammox are significant pathways that remove nitrate as gaseous products from ecosystems,
59 thus reducing the risk of eutrophication. In contrast, DNRA is an alternative pathway that
60 reduces nitrate and nitrite to ammonium. It is a significant, but often overlooked processes in
61 coastal benthic sediments accounting for up to 30% of nitrate reduction activity (Giblin *et al.*,
62 2013). DNRA may contribute to eutrophication by retaining biologically available nitrogen
63 within the system as NH_4^+ . Thus the balance between the two predominant nitrate reduction
64 pathways of denitrification and DNRA in benthic estuarine sediments influence the nutrient
65 load entering costal waters.

66 Both denitrification and DNRA compete for NO_3^- and NO_2^- as an electron acceptor.
67 Nitrogen transformations by denitrification and DNRA in estuarine sediments are influenced
68 by interactions between a number of factors, primarily NO_3^- and organic carbon
69 concentrations, temperature and pH. Previous studies in estuarine sediments have indicated
70 that denitrification may be favoured when nitrate concentrations are high while DNRA tends
71 to outcompete denitrification where there is high availability of organic electron donor and
72 low nitrate (King and Nedwell 1985, Dong *et al.*, 2011).

73 Denitrification and DNRA are catalyzed by a series of nitrate and nitrite reductase
74 enzymes encoded by genes whose abundance can be used as proxies in determining potential
75 for nitrate reduction within environments (Philippot and Hallin 2005). *narG* and *napA* genes

76 encode subunits of two distinct nitrate reductases (NAR and NAP) that mediate reduction of
77 nitrate to nitrite. Nitrite can enter the denitrification pathway in processes mediated by nitrite
78 reductase enzymes encoded by *nirS* or *nirK* genes (see Zumft 1997). Alternatively, in DNRA
79 nitrite is reduced to NH_4^+ by the NrfA enzyme encoded by *nrfA* (see Simon 2002).
80 Consequently, molecular analyses of *nirS/nirK* and *nrfA* genes can be used to investigate the
81 genetic potential in an environment for either denitrification or DNRA.

82 Previously, we demonstrated a decline in rates of denitrification and DNRA, and a
83 corresponding decline in abundance of genetic markers for these processes, down the nitrate
84 gradient of the Colne estuary (Dong *et al.*, 2009) at a single time point (February 2005).
85 Furthermore, previous research revealed seasonal variability in rates of denitrification (Dong
86 *et al.*, 2000); and spatial variability in rates of nitrate exchange across the sediment/water
87 interface, with highest rates in the upper Colne estuary and lowest at the mouth (Thornton *et*
88 *al.*, 2007). These studies did not however simultaneously study the fate of nitrate via benthic
89 denitrification or DNRA nor the nitrate and nitrite reducing communities driving these
90 processes over an annual period to determine seasonal effects. Therefore the aim of this study
91 was to determine rates of nitrate reduction processes linked to corresponding functional gene
92 and transcript abundances along the Colne estuary at two monthly intervals over a 12-month
93 period. Based on previous studies we propose the following hypotheses: first, the trend of
94 decreasing rates of denitrification and DNRA along the estuary gradient is seasonally stable.
95 Second, the relative importance of denitrification and DNRA will vary seasonally, with
96 DNRA higher in the summer. Third, that the abundance of key functional genes and
97 transcripts will correlate spatially and seasonally with corresponding rate processes along the
98 estuary.

99

100 MATERIALS AND METHODS

101 SITE DESCRIPTION, FIELD SAMPLING AND NUTRIENT ANALYSIS

102 Three sites along the Colne estuary, U.K. the estuary head (EH) at the Hythe, mid-
103 estuary (ME) at Alresford Creek and the estuary mouth (EM) at Brightlingsea were sampled
104 at two-monthly intervals from April 2005 to February 2006. The EH is characterised by fine
105 silt sediments (87 to 98% silt:clay <65 μM) and salinity range between 2 to 17 ppt; ME
106 sediments are fine silt (80 – 95% silt:clay <65 μM), with salinity range between 20-32 ppt
107 while EM sediments are clay with a thin layer of fine mud sand (silt:clay <65 μM) and
108 salinity ranging from 28 to 32 ppt. At each site replicate small cores of sediment (10 cm
109 length in core tubes, 3.4 cm internal diameter by 22 cm length) were taken to measure process
110 rates ($n = 5$ per each process). Triplicate sediment samples were also taken from the top 1 cm
111 of sediment for molecular analysis, and returned on ice to the laboratory within one hour of
112 sampling, prior to storage at $-70\text{ }^{\circ}\text{C}$ of aliquots (0.5 g wet weight) of sediment. Water samples
113 were also collected at high tide at the three sites, then samples (10 ml) were filtered through
114 glass fibre filter papers (GF/F, Whatman, UK) and frozen at $-20\text{ }^{\circ}\text{C}$ prior to subsequent
115 colorimetric nutrient analyses (Strickland and Parsons, 1972) using a segmented flow
116 autoanalyser (Skalar Analytical B.V., Breda, The Netherlands). Limits of detection for nitrate
117 and nitrite were $0.002\text{ }\mu\text{M}$, ammonium $0.003\text{ }\mu\text{M}$. Analytical accuracy for nutrient analysis
118 was maintained by membership of a quality assurance scheme (www.quasimeme.org).

119

120 MEASUREMENT OF RATES OF DENITRIFICATION AND DNRA

121 Denitrification rates to both N_2 and N_2O (Dong *et al.*, 2006) and DNRA rates (Dong *et*
122 *al.*, 2009) were determined simultaneously on intact sediment cores. Briefly, denitrification
123 and DNRA rates were measured by ^{15}N -labeled nitrate addition to sediment cores. Five cores
124 of sediment (~ 10 cm deep) were collected in Perspex tubes (3.4 cm internal diameter, 22 cm
125 length) from each site. On return to the laboratory, the cores were put in an incubation tank at

126 *in situ* water temperature and submerged in site water that was vigorously bubbled with air
127 overnight to re-equilibrate. Next day, the rates of denitrification and DNRA were measured
128 by ¹⁵N labeled nitrate addition to sediment cores. After a 3-hour incubation of the cores, the
129 sediment core and the overlying water were mixed to form a slurry. Slurry samples (12.5 ml)
130 were removed for the quantification of denitrification gaseous products (N₂ and N₂O).
131 Subsamples (10 ml) of the slurried sediment cores were taken for the subsequent recovery of
132 ¹⁵NH₄⁺ to determine rates of DNRA. Ammonium in the slurry samples was extracted by
133 steam distillation and ammonium gas was trapped in acid solution. Ammonium in the acid
134 solution was then absorbed onto zeolite, which was then combusted and reduced to N₂.
135 Isotope ratios of N₂ in samples were measured by isotope ratio mass spectrometry using the
136 ^{14:15}N₂ ratio in air as a standard. DNRA rates were calculated using the isotope ratio of N₂.
137 The DNRA calculation in the previous (Dong *et al.*, 2009; Dong *et al.*, 2011) and present
138 work used the ratios of ^{14:15}NO₃⁻ in the water column, thus showing only the rate of DNRA
139 supported by nitrate from the water column.

140

141 NUCLEIC ACID EXTRACTION

142 DNA and RNA were co-extracted from 0.5 g sediment, using Lysing Matrix B tubes
143 (Bio-101) as described previously in Smith *et al.*, (2007). Briefly, to each 0.5 g sediment
144 sample, 0.5 ml of 240 mM sodium phosphate buffer (pH 8) and 0.5 ml of
145 phenol:chloroform:isoamyl alcohol (25:24:1) (pH 4) were added. Samples were lysed by bead
146 beating for 30 seconds at 2,000 rpm, and centrifuged for 10 mins at 17,563 x g. The aqueous
147 phase was added to 0.5 ml chloroform:isoamyl (24:1), mixed and centrifuged for a further 10
148 minutes at 17,563 x g. The aqueous phase was removed for DNA and RNA precipitation with
149 2.5 volumes of ice-cold ethanol and 1/10 volume of 3 M sodium acetate (pH 5.2). Total
150 nucleic acids were pelleted by centrifugation and washed twice in ice cold 70% ethanol, air

151 dried and suspended in 100 µl of DEPC water. Total RNA was prepared by diluting a 25 µl
152 aliquot of total nucleic acids with an equal volume of DEPC-treated sterile water, followed by
153 digestion using TURBO DNA-free (Ambion, Austin, Texas, USA) in accordance with the
154 manufacturer's protocol.

155

156 16S RIBOSOMAL RNA GENE T-RFLP ANALYSIS, CLONE LIBRARY CONSTRUCTION AND Q-PCR 157 ANALYSIS

158 For Terminal Restriction Fragment Length Polymorphism (T-RFLP) analysis, PCR
159 amplification of 16S rRNA genes from DNA was carried out with the primers FAM 63F (5'
160 CAGGCCTAACACATGGCAAGTC '3) (Marchesi *et al.*, 1998) and 518R (5'
161 CGTATTACCGCGGCTGCTCG '3) (Lane 1991). 50 µl reactions contained 0.4 µM forward
162 and reverse primer, 0.1 mM dNTPs, 2.5U *Taq* polymerase, 5 µl of the reaction buffer
163 supplied with the enzyme (Qiagen, Crawley, UK), and 1 µl of 10⁻¹ dilution of DNA template.
164 PCR amplification was carried out in an ABI 2720 Thermo-cycler (Applied Biosystems,
165 Warrington, UK) as follows; 95 °C for 2 min then 30 cycles of 95 °C for 45 sec, 55 °C for 1
166 min and 72 °C for 30 sec and a final extension step of 72 °C for 10 min.

167 Amplified 16S rRNA genes were purified by using a Qiagen PCR purification kit (Qiagen,
168 Crawley, UK) according to the manufacturer's protocol and subsequently independently
169 digested with *AluI* and *CfoI* (Roche Diagnostics, Basel, Switzerland) at 37°C for 3 hours. 5 µl
170 of each digest was desalted; glycogen (20 mg ml⁻¹) (Thermo Scientific, Waltham,
171 Massachusetts, USA) was added to a final concentration of 0.1 µg/ml and ethanol precipitated
172 with 1/10 volume of 3M sodium acetate (pH 5.2) and 2 volumes of ice-cold ethanol. 0.5 µl of
173 the desalted digestion reaction was added to 9.5 µl of deionised formamide and 0.5 µl ROX-
174 labelled Genescan 500 internal size standard (both Applied Biosystems, Warrington, UK).
175 Samples were denatured at 94 °C for 5 min, cooled on ice and separated on an ABI 3700

176 (Applied Biosystems, Warrington, UK) using a 10 second injection and a 8.5 kV separation
177 voltage.

178 Quantitative PCR was used to quantify 16S rRNA genes in sediments using an ABI
179 Prism 7000 detection system as described by Smith *et al.* (2006) using the primers 1369F and
180 1492R and the *TaqMan* probe TM1389F (table 1).

181

182 Q-(RT)-PCR OF NITRATE AND NITRITE REDUCATES GENES AND TRANSCRIPTS

183 Nitrate reductase genes (*narG* and *napA*) and nitrite reductase (*nirS* and *nrfA*) genes
184 and transcripts were quantified from triplicate sediment samples from each site using Q-(RT)-
185 PCR *TaqMan* assays as described in Smith *et al.*, (2007 & 2006). Briefly, *TaqMan* primer and
186 probe sets targeting two *narG* (*narG*-1 & 2), three *napA* (*napA*-1, 2 & 3), three *nirS* (*nirS*-ef,
187 *nirS*-m, *nirS*-n) and a single *nrfA* phylotype were targeted as genetic markers of nitrate
188 reduction, denitrification and DNRA, respectively. *nirK* was targeted but it was not detected
189 along the estuary at any of the time points in question (data not shown). For transcript
190 quantification, *narG*-1 and *nirS*-ef gene transcripts were targeted at the EH and ME sites only
191 based on results of our earlier study (Dong *et al.*, 2009). Details of primer and probe
192 sequences are provided in table 1. Gene and transcript abundances were calculated from
193 standard curves (table 2).

194

195 STATISTICAL ANALYSES

196 T-RFLP profiles were aligned on the basis of T-RF size in base pairs and the
197 individual peak areas of the T-RFs identified by using T-Align (Smith *et al.*, 2005) based on a
198 0.5-bp moving average, resulting in the generation of datasets of aligned T-RFs that gave
199 individual relative peak areas as a proportion (%) of the overall profile. All T-RFs that
200 contributed less than 1% of the total peak area for a profile were excluded from further

201 analysis. The aligned T-RFs were transformed by $\log(X+1)$ to remove any weighting from
202 dominant peaks and analyzed with a Bray-Curtis similarity matrix (Clarke *et al.* 2006) in
203 Primer v6 (Primer-E, Plymouth, United Kingdom). The resultant similarity matrix was
204 analyzed in a two-dimensional multidimensional scaling (MDS) plot.

205 Variation in nitrate reduction rates or gene abundances between sites and within sites
206 at different months were analysed using a one-way ANOVA followed by a post hoc Tukey
207 test (Tukey, 1953) in SPSS v14. Data was $\log(x + 1)$ transformed, as necessary. Spearman's
208 rank correlation analysis was performed to investigate correlations between denitrification or
209 DNRA rates and gene abundances of corresponding genetic determinants in SPSS. A Bray-
210 Curtis resemblance matrix (Clarke *et al.*, 2006) of quantitative PCR gene abundances was
211 generated from the $\log(x+1)$ transformed data and an Euclidean distance resemblance matrix
212 was constructed from rate process data and nutrient concentrations and used to construct
213 multidimensional scaling plots (MDS). Variation among sites was assessed using ANOSIM a
214 one-way analysis of similarity in Primer-6 (Clarke, 1993). BIO-ENV and LINKTREE were
215 used to link gene abundance patterns with rate process and nutrient data. Seasonal trajectories
216 were added to MDS plots by ordering sampling months numerically using the overlay
217 trajectory function within PRIMER-6. MDS, ANOSIM, BIO-ENV and LINKTREE analysis
218 were carried out in Primer 6 (PRIMER-E Ltd, Plymouth Marine Laboratory, UK).

219

220 **RESULTS**

221 **IN SITU NITRATE CONCENTRATIONS AND WATER TEMPERATURE**

222 Nitrate concentrations in water decreased from the estuary head (EH) to estuary mouth
223 (EM) with an annual mean (\pm SE) of $399.7 \pm 50.0 \mu\text{M}$ at EH, $98.8 \pm 23.4 \mu\text{M}$ at ME and 43.1
224 $\pm 10.2 \mu\text{M}$ at EM. (NO_3^- and NH_4^+ concentrations for individual months are shown in figure

225 1). Water temperatures varied seasonally ranging from 4 °C to 19 °C (in February and August
226 respectively).

227

228 **SPATIAL AND TEMPORAL VARIATION IN RATES OF BENTHIC DENITRIFICATION AND DNRA.**

229 Rates of benthic denitrification decreased from the head towards the mouth of the
230 estuary (Figure 1) following the nitrate concentration gradient in the water column. At the
231 estuary head, the mean (\pm SE) annual rate of denitrification ($415.6 \pm 131.2 \mu\text{mol N m}^{-2} \text{h}^{-1}$)
232 was significantly higher (ANOVA, $P < 0.05$) than mid-estuary ($53.1 \pm 16.1 \mu\text{mol N m}^{-2} \text{h}^{-1}$)
233 and the estuary mouth ($12.3 \pm 8.2 \mu\text{mol N m}^{-2} \text{h}^{-1}$), while the latter two did not differ
234 significantly from each other (Figure 1; $P = 0.388$). Mean annual rates of DNRA at the EH
235 ($679.1 \pm 226.9 \mu\text{mol N m}^{-2} \text{h}^{-1}$) and ME ($516.5 \pm 230.1 \mu\text{mol N m}^{-2} \text{h}^{-1}$) did not differ
236 significantly from each other ($P > 0.05$) but were significantly higher (Figure 3, $P < 0.05$)
237 than at EM ($106.3 \pm 37.2 \mu\text{mol N m}^{-2} \text{h}^{-1}$). Rates of denitrification and DNRA at all three
238 sites showed significant seasonal variability ($P < 0.05$, Figure 3). At each site, benthic rates of
239 denitrification were greater than DNRA in April and June only. Rates of DNRA were greater
240 than denitrification at all sites in August, October, December and February (Figure 1).

241

242 **SPATIAL AND TEMPORAL VARIATION IN 16S rRNA COMMUNITY STRUCTURE, ABUNDANCE** 243 **AND DIVERSITY**

244 Changes in community structure along the estuary over the year were assessed by 16S
245 rRNA gene T-RFLP analysis. The results of a Bray-Curtis similarity matrix of T-RFLP
246 profiles generated in triplicate from each site along the estuary over the year revealed two
247 distinct clusters (Figure 2), with the EH forming a separate cluster from the lower estuary
248 sites of ME and EM which were more similar to each other than to the EH (Figure 2). This
249 separation were supported by ANOSIM analysis: EH verses ME $R = 0.58$, $P < 0.001$, EH

250 verses EM $R = 0.913$, $p < 0.001$ and ME verses EM $R = 0.218$, $p < 0.001$. At the EH a
251 sequential seasonal shift in community structure was observed as illustrated by the trajectory
252 (Figure 2), but seasonal cycles in community structure were not evident at the other two sites.
253 16S rRNA gene abundances at each site from April 2005 to February 2006 (Figure 3)
254 indicated a significant site and time effect (2 way ANOVA, $P < 0.001$). Gene abundances were
255 highest at the estuary head and significantly higher than in sediments from mid-estuary and
256 the estuary mouth ($P < 0.001$); while there were no significant differences between ME and
257 EM sediments ($P = 0.071$). Within individual sites, there was only significant variation in 16S
258 rRNA gene copy abundances between months at ME in October (ANOVA $P < 0.008$,
259 Bonferroni correction).

260

261 **SPATIAL AND TEMPORAL VARIATION IN THE ABUNDANCE OF NITRATE REDUCTASE (*narG***
262 **AND *napA*) AND NITRITE REDUCTASE (*nirS* AND *nrfA*) GENES.**

263 In our previous study of the Colne estuary, a suite of nine *TaqMan* primer and probe
264 sets were designed targeting indigenous nitrate and nitrite reducing phylotypes present (Smith
265 *et al.*, 2007). These included two *narG* (*narG*-1 & 2), three *napA* (*napA*-1, 2 & 3), three *nirS*
266 (*nirS*-e, m and n) and one *nrfA* (*nrfA*-2) gene targets. Nitrate (Figure 4) and nitrite (Figure 5)
267 reductase gene abundances were greatest at the estuary head and lowest at the estuary mouth
268 ($P < 0.05$) for eight of the nine phylotypes. The *napA*-3 phylotype was the exception, with
269 no significant difference in gene abundances observed along the estuary ($P < 0.05$). Within
270 individual sites there was only limited temporal variability in gene abundances for both nitrate
271 and nitrite reductase phylotypes (Figure 4 and 5).

272 Percentage relative abundance of nitrate- and nitrite- reducing functional gene
273 abundances to 16S rRNA gene abundances were calculated for each phylotype (Figure 6). In
274 general the highest relative abundance of nitrate- or nitrite-reducing functional gene

275 abundances to 16S rRNA gene abundances were observed at the estuary head (Figure 6)
276 indicating this site as having not only the most abundant bacterial community but also the
277 highest proportion of nitrate reducers in that community: commensurate with the highest
278 nitrate concentrations along the estuary. Exceptions to this trend were the *narG*-1 and *napA*-3
279 phlotypes, which were greatest at ME and EM sites respectively. For all genes a peak in
280 relative abundance was observed at the EH in February 2006 corresponding to a peak in
281 nitrate and ammonium concentrations (Figure 3).

282

283 **SPATIAL AND TEMPORAL VARIATION IN *narG* AND *nirS* GENE TRANSCRIPTION.**

284 Trends of transcript abundances reflected those observed at the DNA level - *narG*
285 transcript abundances were highest at the estuary head, while differences in *nirS*-ef transcripts
286 numbers were not observed between sites (Figure 7, $P > 0.05$).

287

288 **INTER-RELATIONSHIPS BETWEEN FUNCTIONAL GENE ABUNDANCES, NITRATE** 289 **CONCENTRATIONS, RATES OF DENITRIFICATION AND DNRA.**

290 An MDS plot of Bray-Curtis square-root transformed mean gene abundances (i.e. four
291 genes; totalling nine phlotypes) at each site from April to February (Figure 8A) shows
292 spatial and temporal variation in the abundance of the nitrate- and nitrite-reductase genes
293 along the estuary. Gene abundances at the EH site clustered separately from those at ME
294 and EM sites. A one-way ANOSIM indicated a significant difference in the abundance of
295 nitrate- and nitrite-reductases genes at the three sites ($R = 0.679$, $P < 0.001$). As with the 16S
296 rRNA community analysis (Figure 2), there was evidence of community change over time
297 (seasonality) at the estuary head in nitrate- and nitrite reductase gene abundances as indicated
298 by the trajectory on Figure 8A. Relationships between gene abundances, denitrification and
299 DNRA rates and nitrate and ammonia concentrations were explored using BIO-ENV and

300 LINKTREE in PRIMER-6 (Clarke and Ainsworth, 1993). BIO-ENV identified nitrate (R=
301 0.639, $p < 0.001$) as the single measured abiotic variable that best explained the clustering of
302 nitrate and nitrite reductase gene abundances along the estuary. To further explore the
303 observed clustering of nitrate and nitrite reductase gene abundances, a LINKTREE non-
304 parametric analysis was conducted in PRIMER6 (Figure 8B), to link the gene abundance
305 clusters to the range of nutrient concentrations or rates of denitrification and DNRA. 3 distinct
306 splits labelled 1, 2 & 3, formed in the LINKTREE dendrogram. The first split was observed
307 between the EH and the lower estuary sites and was defined by NO_3^- concentrations > 202
308 μM . All other sites, fell into split 2 where NO_3^- concentrations were $< 146 \mu\text{M}$. The next split
309 separated the EM site in August from the rest based on the lowest observed nitrate
310 concentration. Split 3, divided EM sites in April, August and October based on denitrification
311 rates $> 71 \mu\text{mol N m}^2 \text{ h}^{-1}$ with remaining sites characterised by rates of denitrification below
312 $< 53 \mu\text{mol N m}^2 \text{ h}^{-1}$.

313 Spearman's correlation co-efficient analysis was performed to examine correlations
314 between rates of denitrification or DNRA and the abundance of their corresponding genetic
315 determinants (Table 3). For denitrification significant weak to strong (correlations absolute
316 value of r range between 0.40 to 0.79) were observed between the rates of denitrification and
317 corresponding abundances of *nirS-n* and *nirS-m* phylotypes. *nirS-n*, *m* and *e* primer and probe
318 sets target *nirS* phylotypes first recovered as mRNA *nirS* gene sequences from sediments at
319 the head of the Colne estuary similar to *nirS* from gamma and alpha proteobacteria (Nogales
320 *et al.*, 2000, Smith *et al.*, 2007). Weak to moderate, but not significant correlations were
321 observed between denitrification and *nirS-e* and DNRA and *nrfA* gene abundances (Table 3).
322 The *nirS-e* primer and probe set target *nirS* gene sequences first retrieved from the mid-
323 estuary site of the Colne as mRNA and phylogenetically group with gamma proteobacteria
324 (Nogales *et al.*, 2000, Smith *et al.*, 2007). The *nrfA* primer set targeted *nrfA* phylotypes

325 retrieved from the Colne estuary head site that phylogenetically group with epsilon-
326 proteobacteria (Smith *et al.*, 2007).

327

328 **DISCUSSION**

329 In this study, we report spatial and temporal dynamics in the activity of benthic nitrate
330 reduction coupled to quantification of nitrate reducing functional genes and transcripts along
331 an estuarine gradient. Denitrification, DNRA and corresponding nitrate and nitrite functional
332 gene abundances decreased along the estuary, following the nitrate gradient in the water
333 column as previously observed in the Colne estuary (Ogilvie *et al.*, 1997, Dong *et al.*, 2009)
334 and the Thames (Trimmer *et al.*, 2000). Denitrification at the estuary head greatly exceeded
335 that of the other sites. At the estuary head, rates of denitrification were highest in June,
336 whereas in the middle of the estuary and at the mouth rates peaked in October. Lowest rates
337 of denitrification at all three sites were observed in December. Our earlier studies of the Colne
338 (Dong *et al.*, 2000) and the Great Ouse (Trimmer *et al.*, 1998) had shown highest
339 denitrification rates during late spring/summer and lowest denitrification activity during the
340 winter.

341 The separation of the estuary head from sites lower down the estuary was not as
342 pronounced when it came to DNRA. Rates of DNRA at the estuary head and middle sites
343 were similar, and DNRA at the middle estuary site was, in fact, greater than at the estuary
344 head in four out of six months (October and February). Seasonal variability was also observed
345 for DNRA, with the highest rates in late summer and early autumn, and lowest rates in spring
346 (Figure 1). Giblin *et al.*, (2010) measured denitrification and DNRA in the Parker River
347 estuary for 13 years at a single upstream site (salinity between 0 and 18 ppt) between 1993
348 and 2006. Large seasonal and inter-annual variation in denitrification and DNRA was
349 reported, primarily driven by salinity not temperature. Rates of DNRA in the Parker River

350 Estuary were highest in late summer (August) and lowest in early spring (March). Spatially,
351 denitrification in the Parker River exhibited the opposite trend to the Colne estuary, as it was
352 inversely related to the salinity gradient with a peak in denitrification in late spring in this
353 estuary. In the Norsminde Fjord, Denmark, Jorgensen (1989) reported two maxima in
354 denitrification, the first in early spring and the second in autumn. A peak in DNRA was
355 observed in late summer, attributed to the more highly reduced sediments within the estuary
356 at this time. The results from the Colne data are in agreement with modelling studies (Kelly-
357 Gerreyn *et al.*, 2001), and data from tropical estuaries (Dong *et al.*, 2011) that suggested
358 DNRA tends to become increasingly important at higher environmental temperatures.

359 Denitrification has in the past been considered the dominant nitrate reduction pathway
360 in coastal and marine sediments and DNRA less important, if considered at all (for a review
361 see Giblin *et al.*, 2013, Burgin and Hamilton 2007). Our previous single time-point study of
362 denitrification, DNRA and anammox, showed that more nitrate was removed from the system
363 via denitrification than was reduced to ammonia by DNRA (Dong *et al.*, 2009). Anammox
364 was detected only at the estuary head and accounted for 30% of the N₂ formation. In this
365 study anammox was not measured, due to logistical limitations, instead focusing on nitrate
366 reduction pathways of denitrification and DNRA. Over the annual time period, denitrification
367 rates exceeded those of DNRA only in the late spring/early summer (April and June) at all
368 three sites along the estuary. For the remainder of the year, at the time points measured, rates
369 of DNRA exceeded those of denitrification indicating that more nitrate was being reduced and
370 converted to ammonia than was being lost from the system in gaseous forms via
371 denitrification. This further highlights the importance of not relying on single time point
372 studies to understand the dynamics of the nitrogen cycle in dynamic estuarine systems.

373 Denitrification and DNRA compete for nitrate and carbon within sediments. The
374 availability of nitrate and organic carbon are key factors controlling rates of benthic

375 denitrification (Cornwell *et al.*, 1999, Dong *et al.*, 2000, Fulweiler and Heiss 2014). Previous
376 studies of the Colne estuary have indicated that denitrification at the estuary head is carbon
377 limited, while denitrification mid-estuary and at the estuary mouth is nitrate limited
378 (Papasprou *et al.*, 2014). However, the ratio of electron donor to acceptor can influence the
379 pathway and fate of nitrate. DNRA has a higher affinity for nitrate than denitrification and
380 may be favoured in nitrate-limited, carbon-rich environments (King and Nedwell 1985,
381 Bergin and Hamilton 2007, Kraft *et al.*, 2014). This is due to the requirement of only 5
382 electrons to reduce nitrate in denitrification versus the 8 required for DNRA (Teidje, 1988).
383 DNRA may therefore outcompete denitrification in nitrate-limited environments where these
384 organisms gain more energy from DNRA than denitrifiers can from denitrification. Indeed
385 nitrate concentrations at the mid-estuary site were much lower than at the estuary head and in
386 the months where DNRA was the dominant process it was 5 to 2120 times greater than
387 denitrification at this site (Alresford). Recent studies in similar environments have shown that
388 DNRA is often the prominent nitrate reduction pathway. For examples, Giblin *et al.*, 2013,
389 showed DNRA was greater than denitrification in 30% of 55 coastal sediments sites
390 examined. Similarly, Song *et al.*, (2014), in a single time point study of benthic DNRA in the
391 New River estuary, North Carolina, USA showed it was responsible for 44 to 74% of nitrate
392 reduction and reported that DNRA rates were greater than denitrification (Lisa *et al.*, 2014).

393 The results of our study have highlighted, for the first time, the importance of DNRA
394 as a significant pathway for benthic sediment nitrate reduction in the Colne estuary. The rates
395 of benthic DNRA of nitrate from the water column (DNRA_w) in the whole estuary was
396 estimated as 11.48 Mmol N yr⁻¹ derived by multiplying the mean annual rates of DNRA at the
397 estuary head (679 μmol N m⁻² h⁻¹), mid-estuary (517 μmol N m⁻² h⁻¹) and estuary mouth
398 (106.7 μmol N m⁻² h⁻¹) by the total area of sediment (which is defined as the 72% of the area
399 totally immersed at spring tide; Ogilvie *et al.*, 1997) in the sector of the river centred around

400 each site (Dong *et al.*, 2000). Using the mass balance approach, by subtracting oxidized
401 inorganic nitrogen ($\text{NO}_3^- + \text{NO}_2^-$) removal by denitrification supported by nitrate from water
402 column ($5.09 \text{ Mmol N yr}^{-1}$) from the total sediment uptake of oxidized inorganic nitrogen
403 ($16.28 \text{ Mmol N yr}^{-1}$), a very similar DNRA rate of $11.19 \text{ Mmol N yr}^{-1}$ was obtained (Thornton
404 *et al.*, 2007).

405 At the molecular level, the abundances of gene and transcript molecular markers for
406 nitrate reduction (*narG* & *napA*), denitrification (*nirS*) and DNRA (*nrfA*) generally showed a
407 consistent overall spatial trend of declining abundances from the estuary head to the estuary
408 mouth (Figures 4, 5 & 6) as observed in the rate process data, supporting and extending our
409 previous studies along the Colne estuary at single time points (Smith *et al.*, 2007, Dong *et al.*,
410 2009). In contrast to our observations in the hypernutrified Colne, *nirS* and *nirK* gene
411 abundances along the lower nutrient Fitzroy estuary, Australia showed no statistical
412 difference between sites, despite some observed variability in the net rates of denitrification
413 along the estuary (Abell *et al.*, 2010). The one exception to this trend of decreasing gene
414 abundances along the estuary was the *napA-3* phylotype (alphaproteobacteria) where gene
415 abundances throughout the 12 month sampling period remained constant along the estuary
416 gradient (Figure 4), suggesting a different selective mechanism and different ecological
417 significance for this *nap* phylotype than for the other two phylotypes (both
418 gammaproteobacteria). While we have determined the distributions of these different
419 functional genes and their phylotypes along the estuary, one of the key questions remaining to
420 be elucidated is the different functions of these phylotypes, which can probably only be
421 clarified by controlled laboratory-based studies. Richardson *et al.*, (2001) suggested that NAR
422 and NAP provide adaptations to different nitrate environments, the former facilitating nitrate
423 reduction in reduced, high nitrate environments whereas NAP is adaptive to effective nitrate
424 scavenging in lower nitrate and less reduced environments. The distributions that we

425 measured along the Colne estuary would suggest that these different *napA* phylotypes,
426 particularly *napA-3* generally support this hypothesis as total bacterial numbers decline along
427 the estuary but *napA* numbers remain high indicating that they are relatively more important
428 at lower nitrate concentrations than *narG*.

429 While gene and transcript abundances generally decreased along the estuary gradients,
430 as observed in the rate process data, finer scale correlations between rates and gene/transcript
431 abundances on temporal scales were not observed. Some studies have shown good agreement
432 between activity measurements and gene and/or transcript abundances e.g. in studies of
433 archaeal nitrification (Wuchter *et al.*, 2006). However there is evidence in the literature to
434 indicate the direct measurement of functional genes at DNA and even mRNA levels can be
435 uncoupled to activity measurements, indicating that substantial post-transcriptional, protein
436 assembly and/or environmental factors ultimately control activity. For example, Ikeda *et al.*,
437 (2009) examined the roles of NAR and NAP in nitrate reduction in *Pseudomonas sp.* and
438 found that nitrate reductase activity and *napA* or *narG* gene transcription were not necessarily
439 positively correlated, leading them to conclude that there were subsequent post-translational
440 modifications even in pure culture. In soils, Liu *et al.*, (2010) demonstrated the dramatic
441 effect increasing pH had on reducing denitrification activity, yet this trend was not
442 reciprocated in *nirS* and *nosZ* gene and transcript abundance, leading them to conclude that
443 reduction in pH affected denitrification after transcription. In the highly nitrified Colne
444 estuary, the high nitrate concentrations in the water are drastically reduced within the surface
445 sediment by rapid nitrate reduction in the sub-oxic zone (the surface oxic layer of sediment is
446 usually <2-3mm depth (Robinson *et al.*, 1998). Consequently, benthic nitrate reducers are
447 operating at very low pore water nitrate concentrations where rates of nitrate reduction
448 approximate to first order kinetics; well below any nitrate-saturating concentrations when
449 nitrate reduction might correlate with genetic potentials. The correspondence between rate

450 processes and gene abundances/transcripts is likely to be closer the nearer *in situ* substrate
451 concentrations are to saturating concentrations of substrates. Furthermore other physical-
452 chemical factors such as temperature or pH may control key enzyme activity, and *in situ* rates,
453 without necessarily directly affecting transcription. Further and future studies will focus on
454 determining the links between environmental conditions, nitrate and nitrite reducing
455 communities and rates of nitrate reduction and controlling factors influencing the fate of
456 nitrate within estuarine sediments.

457

458

459 **ACKNOWLEDGEMENTS**

460 We thank John Green for excellent technical support in field sampling and in processing
461 stable isotope samples. This work was supported by the Natural Environment Research
462 Council of the United Kingdom through research grant NER/A/S/2002/00962 awarded to
463 D.B.N and A.M.O. CJS is currently supported by SFI Starting Investigator-COFUND
464 fellowship (11/SIRG/B2159).

465 **REFERENCES**

- 466 Abell, G. C. J., Revill, A. T., Smith, C., Bissett, A. P., Volkman, J. K., and Robert, S. S.
 467 (2009). Archaeal ammonia oxidizers and *nirS*-type denitrifiers dominate sediment
 468 nitrifying and denitrifying populations in a subtropical macrotidal estuary. *ISME J.* 4,
 469 286–300. doi:10.1038/ismej.2009.105.
- 470 Brin, L. D., Giblin, A. E., and Rich, J. J. (2014). Environmental controls of anammox and
 471 denitrification in southern New England estuarine and shelf sediments. *Limnol. Oceanogr.*
 472 59, 851–860. doi:10.4319/lo.2014.59.3.0851.
- 473 Burgin, A. J., and Hamilton, S. K. (2007). Have we overemphasized the role of denitrification
 474 in aquatic ecosystems? A review of nitrate removal pathways. *Front. Ecol. Environ.* 5,
 475 89–96. doi:10.1890/1540-9295 [89:HWOTRO]2.0.CO;2.
- 476 Clarke, K. R. (1993). Non-parametric multivariate analyses of changes in community
 477 structure. *Aust. J. Ecol.* 18, 117–143. doi:10.1111/j.1442-9993.1993.tb00438.x.
- 478 Clarke, K. R., and Ainsworth, M. (1993). A method of linking multivariate community
 479 structure to environmental variables. *Mar. Ecol. Prog. Ser.* 92, 205–219.
 480 doi:10.3354/meps092205.
- 481 Clarke, K. R., Somerfield, P. J., and Chapman, M. G. (2006). On resemblance measures for
 482 ecological studies, including taxonomic dissimilarities and a zero-adjusted Bray–Curtis
 483 coefficient for denuded assemblages. *J. Exp. Mar. Biol. Ecol.* 330, 55–80.
 484 doi:10.1016/j.jembe.2005.12.017.
- 485 Cornwell, J. C., Kemp, W. M., and Kana, T. M. (1999). Denitrification in coastal ecosystems:
 486 methods, environmental controls, and ecosystem level controls, a review. *Aquat. Ecol.* 33,
 487 41–54. doi:10.1023/A:1009921414151.
- 488 Dong, L. F., Thornton, D., and Nedwell, D. B. (2000). Denitrification in sediments of the
 489 River Colne estuary, England. *Mar. Ecol. Prog. Ser.* 203,109–122
 490 *d.o.i:10.3354/meps203109*
- 491 Dong, L. F., Nedwell, D. B., Underwood, G. J. C., Thornton, D. C. O., and Rusmana, I.
 492 (2002). Nitrous oxide formation in the Colne estuary, England: the central role of nitrite.
 493 *Appl. Environ. Microbiol.* 68, 1240–1249. doi:10.1128/AEM.68.3.1240-1249.2002.
- 494 Dong, L. F., Nedwell, D. B., and Stott, A. (2006). Sources of nitrogen used for denitrification
 495 and nitrous oxide formation in sediments of the hypernutrified Colne, the nutrified
 496 Humber, and the oligotrophic Conwy estuaries, United Kingdom. *Limnol. Oceanogr.* 51,
 497 545–557. doi:10.4319/lo.2006.51.1_part_2.0545.
- 498 Dong, L. F., Smith, C. J., Papaspyrou, S., Stott, A., Osborn, A. M., and Nedwell, D. B.
 499 (2009). Changes in benthic denitrification, nitrate ammonification, and anammox process
 500 rates and nitrate and nitrite reductase gene abundances along an estuarine nutrient
 501 gradient (the Colne estuary, United Kingdom). *Appl. Environ. Microbiol.* 75, 3171–3179.
 502 doi:10.1128/AEM.02511-08.
- 503 Dong, L. F., Sobey, M. N., Smith, C. J. Rusmana, I., Phillips, W., Stott, A., Osborn, A.M.,

- 504 Nedwell, D.B. (2011). Dissimilatory reduction of nitrate to ammonium, not denitrification
505 or anammox, dominates benthic nitrate reduction in tropical estuaries. *Limnol. Oceanogr.*
506 *56*, 279-291 doi:10.4319/lo.2011.56.1.0279.
- 507 Earl, T.J., Upton, G.J.G, Nedwell, D.B. (2014) UK catchments nutrient loads 1993-2003, a
508 new approach using harmonised monitoring scheme data: temporal changes, geographical
509 distribution, limiting nutrients and loads to coastal waters. *Environ. Sci. Process. Impact.*
510 *16*, 1646-1658. doi: 10.1039/c4em00021h.
- 511 Fulweiler, R., and Heiss, E. (2014). (Nearly) A Decade of Directly Measured Sediment N₂
512 Fluxes: What Can Narragansett Bay Tell Us About the Global Ocean Nitrogen Budget?
513 *Oceanog.* *27*, 184–195. doi:10.5670/oceanog.2014.22.
- 514 Giblin, A. E., Tobias, C. R., Song, B., Weston, N., and Banta, G. T. (2013). The importance
515 of dissimilatory nitrate reduction to ammonium (DNRA) in the nitrogen cycle of coastal
516 ecosystems. *Oceanography* *26*, 124-131
- 517 Giblin, A. E., Weston, N. B., Banta, G. T., Tucker, J., and Hopkinson, C. S. (2010). The
518 effects of salinity on nitrogen losses from an oligohaline estuarine sediment. *Estuaries*
519 *and Coasts* *33*, 1054–1068. doi:10.1007/s12237-010-9280-7.
- 520 Ikeda, E., Andou, S., Iwama, U., Kato, C., Horikoshi, K., and Tamegai, H. (2009).
521 Physiological roles of two dissimilatory nitrate reductases in the deep-sea denitrifier
522 *Pseudomonas sp.* strain MT-1. *Biosci. Biotechnol. Biochem.* *73*, 896–900.
523 doi:10.1271/bbb.80833.
- 524 Jørgensen, K. S. (1989). Annual pattern of denitrification and nitrate ammonification in
525 estuarine sediment. *Appl. Environ. Microbiol.* *55*, 1841–1847.
526
- 527 Kelly-Gerreyn, B. A., Trimmer, M., and Hydes, D. J. (2001). A diagenetic model
528 discriminating denitrification and dissimilatory nitrate reduction to ammonium in a
529 temperate estuarine sediment. *Mar. Ecol. Prog. Ser.* *220*, 33–
530 46. doi:10.3354/meps220033
- 531 King, D., and Nedwell, D. B. (1985). The influence of nitrate concentration upon the end-
532 products of nitrate dissimilation by bacteria in anaerobic salt marsh sediment. *FEMS*
533 *Microbiol. Ecol.* *1*, 23–28. doi:10.1111/j.1574-6968.1985.tb01127.x.
- 534 Kraft, B., Tegetmeyer, H. E., Sharma, R., Klotz, M. G., Ferdelman, T. G., Hettich, R. L.,
535 Geelhoed, J. S., and Strous, M. (2014). The environmental controls that govern the end
536 product of bacterial nitrate respiration. *Science* *345*, 676–679.
537 doi:10.1126/science.1254070.
- 538 Kuenen, J. G. (2008). Anammox bacteria: from discovery to application. *Nat. Rev. Micro.* *6*,
539 320–326. doi:10.1038/nrmicro1857.
- 540 Lane, D. J. (1991). "16S/23S rRNA sequencing", in *Nucleic acid techniques in bacterial*
541 *systematics*. Eds Stackebrandt E., Goodfellow M. (John Wiley & Sons, Chichester,
542 United Kingdom), pp 115–175.
- 543 Lisa, J. A., Song, B., Tobias, C. R., and Duernberger, K. A. (2014). Impacts of freshwater
544 flushing on anammox community structure and activities in the New River Estuary, USA.

- 545 *Aquat. Microb. Ecol.* 72, 17–31. doi:10.3354/ame01682.
- 546 Liu, B., Mørkved, P. T., Frostegård, Å., and Bakken, L. R. (2010). Denitrification gene pools,
547 transcription and kinetics of NO, N₂O and N₂ production as affected by soil pH. *FEMS*
548 *Microbiol. Ecol.* 72, 407–417. doi:10.1111/j.1574-6941.2010.00856.x.
- 549 Lozupone, C. A., and Knight, R. (2007). Global patterns in bacterial diversity. *PNAS* 104,
550 11436–11440. doi:10.1073/pnas.0611525104.
- 551 Marchesi, J. R., Sato, T., and Weightman, A. J. (1998). Design and evaluation of useful
552 bacterium-specific PCR primers that amplify genes coding for bacterial 16S rRNA. *Appl.*
553 *Environ. Microbiol.* 64, 795–799
- 554 Nedwell, D. B., Jickells, T. D., Trimmer, M., and Sanders, R. (1999). “Nutrients in
555 Estuaries,” in *Estuaries Advances in Ecological Research*. (Elsevier), 43–92.
556 doi:10.1016/S0065-2504(08)60191-9.
- 557 Nedwell, D. B., Dong, L. F., Sage, A., and Underwood, G. J. C. (2002). Variations of the
558 nutrients loads to the mainland U.K. estuaries: Correlation with catchment areas,
559 urbanization and coastal eutrophication. *Estuar. Coast. Mar. Sci.* 54, 951–970.
560 doi:10.1006/ecss.2001.0867.
- 561 Nicholls, J. C., and Trimmer, M. (2009). Widespread occurrence of the anammox reaction in
562 estuarine sediments. *Aquat. Microb. Ecol.* 55, 105–113. doi:10.3354/ame01285.
- 563 Nogales, B., Timmis, K. N., Nedwell, D. B., and Osborn, A. M. (2002). Detection and
564 Diversity of Expressed Denitrification Genes in Estuarine Sediments after Reverse
565 Transcription-PCR Amplification from mRNA. *Appl. Environ. Microbiol.* 68, 5017–
566 5025. doi:10.1128/AEM.68.10.5017-5025.2002.
- 567 Ogilvie, B., Nedwell, D. B., Harrison, R. M., Robinson, A., and Sage, A. (1997). High nitrate,
568 muddy estuaries as nitrogen sinks: the nitrogen budget of the River Colne estuary (United
569 Kingdom). *Mar. Ecol. Prog. Ser.* 150, 217–228. doi:10.3354/meps150217.
- 570 Philippot, L., and Hallin, S. (2005). Finding the missing link between diversity and activity
571 using denitrifying bacteria as a model functional community. *Curr. Opin. Microbiol.* 8,
572 234–239. doi:10.1016/j.mib.2005.04.003.
- 573 Richardson, D. J., Berks, B. C., Russell, D. A., Spiro, S., and Taylor, C. J. (2001). Functional,
574 biochemical and genetic diversity of prokaryotic nitrate reductases. *Cell. Mol. Life Sci.*
575 58, 165–178.
- 576 Robinson, A. D., Nedwell, D. B., Harrison, R. M., and Ogilvie, B. G. (1998). Hypernutrified
577 estuaries as sources of N₂O emission to the atmosphere: the estuary of the River Colne,
578 Essex, UK. *Mar. Ecol. Prog. Ser.* 164, 59–71. doi:10.3354/meps164059.
- 579 Seitzinger, S. P. (1988). Denitrification in freshwater and coastal marine ecosystems:
580 Ecological and geochemical significance. *Limnol. Oceanogr.* 33, 702–724.
581 doi:10.4319/lo.1988.33.4part2.0702.
- 582 Simon, J. (2002). Enzymology and bioenergetics of respiratory nitrite ammonification. *FEMS*
583 *Microbiol Rev* 26, 285–309. doi:10.1111/j.1574-6976.2002.tb00616.x/full.

- 584 Smith, C. J., Danilowicz, B. S., Clear, A. K., Costello, F. J., Wilson, B., and Meijer, W. G.
585 (2005). T-Align, a web-based tool for comparison of multiple terminal restriction
586 fragment length polymorphism profiles. *FEMS Microbiol. Ecol.* 54, 375–380.
587 doi:10.1016/j.femsec.2005.05.002.
- 588 Smith, C. J., Nedwell, D. B., Dong, L. F., and Osborn, A. M. (2007). Diversity and abundance
589 of nitrate reductase genes (*narG* and *napA*), nitrite reductase genes (*nirS* and *nrfA*), and
590 their transcripts in estuarine sediments. *Appl. Environl. Microbiol.* 73, 3612–3622.
591 doi:10.1128/AEM.02894-06.
- 592 Smith, C. J., Nedwell, D. B., Dong, L. F., and Osborn, A. M. (2006). Evaluation of
593 quantitative polymerase chain reaction-based approaches for determining gene copy and
594 gene transcript numbers in environmental samples. *Environ. Microbiol.* 8, 804–815.
595 doi:10.1111/j.1462-2920.2005.00963.x.
- 596 Song, B., Lisa, J. A., and Tobias, C. R. (2014). Linking DNRA community structure and
597 activity in a shallow lagoonal estuarine system. *Front. Microbiol.* 5.
598 doi:10.3389/fmicb.2014.00460.
- 599 Strickland, J. D. H., and PARSONS, T. R. 1972. A practical handbook of seawater analysis,
600 2nd ed. Fisheries Research Board of Canada, 310 pp, Ottawa.
601
- 602 Strous, M., Fuerst, J. A., Kramer, E. H., Logemann, S., Muyzer, G., van de Pas-Schoonen, K.
603 T., Webb, R., Kuenen, J. G., and Jetten, M. S. (1999). Missing lithotroph identified as
604 new planctomycete. *Nature* 400, 446–449. doi:10.1038/22749.
- 605 Thornton, D., Dong, L. F., and Underwood, G. (2007). Sediment-water inorganic nutrient
606 exchange and nitrogen budgets in the Colne Estuary, UK. *Mar. Ecol. Prog. Ser.* 337, 63-
607 77. doi:10.3354/meps337063.
- 608 Tiedje, J. M. (1988). "Ecology of denitrification and dissimilatory nitrate reduction to
609 ammonium," in *Environmental Microbiology of Anaerobes* (New York: Biology of
610 anaerobic microorganisms), 179–244.
- 611 Trimmer, M., Nedwell, D. B., Sivyer, D. B., and Malcolm, S. J. (1998). Nitrogen fluxes
612 through the lower estuary of the river Great Ouse, England: the role of the bottom
613 sediments. *Mar. Ecol. Prog. Ser.* 163, 109–124. doi:10.3354/meps163109.
- 614 Trimmer, M., Nedwell, D. B., Sivyer, D. B., & Malcolm, S. J. (2000). Seasonal benthic
615 organic matter mineralisation measured by oxygen uptake and denitrification along a
616 transect of the inner and outer River Thames estuary, UK. *Mar. Ecol. Prog. Ser.* 197,
617 103–119. doi:10.3354/meps197103
- 618 Tukey, J.W. (1953). "The collected works of John W. Tukey, vol. 3." in *Multiple comparisons*
619 (Chapman and Hall, New York, NY.) p1948-1983.
- 620 Wuchter, C., Abbas, B., Coolen, M. J. L., Herfort, L., van Bleijswijk, J., Timmers, P., Strous,
621 M., Teira, E., Herndl, G. J., Middelburg, J. J., et al. (2006). Archaeal nitrification in the
622 ocean. *PNAS* 103, 12317–12322. doi:10.1073/pnas.0600756103.
- 623 Zumft, W. G. (1997). Cell biology and molecular basis of denitrification. *Microbiol. Mol.*

625

626 **TITLES AND LEGENDS TO FIGURES**

627 **Figure 1.** Temporal and spatial variation in top: Nitrate and ammonium concentrations and
628 bottom: Rates (+/- SE, n=5) of (A) Denitrification and (B) DNRA in sediments along the
629 Colne estuary sampled from April 2005 to February 2006. For each process, significant
630 differences in the overall process rates between sites along the estuary are indicated by
631 different Greek letters above the letters above coloured lines (black = estuary head (EH), red
632 = mid-estuary (ME) and blue = estuary mouth, EM))

633

634 **Figure 2.** Non-metric Multi-Dimensional Scaling plot of total community T-RFLP profiles
635 from three sites along the estuary sampled at two-monthly intervals from April 2005 to
636 February 2006. Each month is represented in biological triplicates and coded according to
637 site. Insert map showing sample location along the Colne estuary. Black triangles represent
638 the estuary head (EH), gray circles mid-estuary (ME) and white squares the estuary mouth
639 (EM). A = April, J = June, Au = August, O = October, D = December, F = February 2006.

640

641 **Figure 3.** Spatial and temporal variation in 16S rRNA gene copy abundances in sediments
642 from the Colne estuary from April 2005 to February 2006. Standard errors (n = 3) are shown.
643 Greek letters above coloured lines (black = estuary head (EH), red = mid-estuary (ME) and
644 blue = estuary mouth (ME)) indicate statistical differences in the overall gene abundances
645 across the year between sites ($p < 0.001$)

646

647 **Figure 4.** Variation in abundance (gene copies g^{-1} sediment +/-SE, n=3) of nitrate reductase
648 genes (*narG* and *napA*) in sediments along the Colne estuary sampled from April 2005 to

649 February 2006. For each phylotype, significant differences in annual gene abundances
650 between sites along the estuary are indicated by different Greek letters above coloured lines
651 (black = estuary head (EH), red = mid-estuary (ME) and blue = estuary mouth (EM))

652

653 **Figure 5.** Variation in abundance (gene copies g^{-1} sediment \pm SE, $n=3$) of nitrite reductase
654 genes (*nirS* and *nrfA*) in sediments along the Colne estuary sampled from April 2005 to
655 February 2006. For each phylotype, significant differences in annual gene abundances
656 between sites along the estuary are indicated by different Greek letters above coloured lines
657 (black = estuary head (EH), red = mid-estuary (ME) and blue = estuary mouth (EM))

658

659 **Figure 6.** Relative abundance (%) of nitrate- and nitrite- reductase phylotype gene
660 abundances to 16S rRNA gene abundances along the estuary over the annual sampling period.

661

662 **Figure 7.** Variation in nitrate (*narG-2*) and nitrite (*nirS-ef*) reductase gene transcript
663 abundances (transcripts g^{-1} sediment \pm SE, $n=3$) in sediments along the Colne estuary
664 sampled from April 2005 to February 2006. For each phylotype, significant differences in
665 annual transcript abundances between sites along the estuary are indicated by different Greek
666 letters above the coloured lines representing each site (black = estuary head (EH), red = mid-
667 estuary (ME)).

668

669 **Figure 8.** A: Non-metric multidimensional scaling (MDS) ordination of a Bray-Curtis
670 resemblance matrix calculated from square-root transformed mean Q-PCR nitrate- and nitrite-
671 reductase gene abundances quantified two-monthly intervals from sediments at each site;
672 temporal variation at the estuary head (EH) is illustrated by a time-line trajectory drawn
673 through sampling time points. (B). LINKTREE analysis of all sites and time points to identify

674 environmental variable range (nitrate, ammonia, denitrification or DNRA) driving clustering
675 of nitrate-nitrite reducing community observed in 8A. Three splits (1 -3) and variable range
676 responsible for the divide are shown. %B, an absolute measure of group difference is shown
677 on the x-axis. ANOSIM R value and *p*-values are reported for each split. Months: A = April, J
678 = June, Au = August, O = October, D = December, F = February (2006)

679

680 **Table 1.** Q- (RT)-PCR primer and probe sets used in this study

681	Target	Primer/probe^a	Sequence (5' - 3')	Amplicon	Annealing
682	(reference)			(bp)	°C
683	16S rRNA	1369F	CGGTGAATACGTTCYCGG	123	56
684	Suzuki <i>et al.</i>	1492R	TACGGYTACCTTGTTACGACTT		
685	(2000)	TM1389F	CTTGTACACACCGCCCGTA		
686	<i>napA-1</i>	<i>napA-1F</i>	GTYATGGARGAAAAATTCAA	111	55
687	Smith <i>et al.</i>	<i>napA-1R</i>	GARCCGAACATGCCRAC		
688	(20007)	<i>napA-1 TM*</i>	AACATGACCTGGAAG		
689	<i>napA-2</i>	<i>napA-2F</i>	GAACCKAYGGGYTGTTATG	76	55
690	Smith <i>et al.</i>	<i>napA-2R</i>	TGCATYTCSGCCATRTT		
691	(20007)	<i>napA-2 TM*</i>	CTTTGGGGTTCAA		
692	<i>napA-3</i>	<i>napA-3F</i>	CCCAATGCTCGCCACTG	130	60
693	Smith <i>et al.</i> ,	<i>napA-3R</i>	CATGTTKGAGCCCCACAG		
694	(2007)	<i>napA-3 TM*</i>	TGGGTTGTTACGA		
695	<i>narG-1</i>	<i>narG-1F</i>	GAC TTC CGC ATG TCR AC	69	60
696	Smith <i>et al.</i>	<i>narG-1R</i>	TTY TCG TAC CAG GTG GC		
697	(2007)	<i>narG-1 TM*</i>	TAYTCCGACATCGT		
698	<i>narG-2</i>	<i>narG-2F</i>	CTCGAYCTGGTGGTYGA	89	55
699	Smith <i>et al.</i>	<i>narG-2R</i>	TTYTCGTACCAGGTSGC		
700	(2007)	<i>narG-2 TM*</i>	AACTTCCGCATGGA		
701	<i>nrfA-2</i>	<i>nrfA-2F</i>	CACGACAGCAAGACTGCCG	67	60
702	Smith <i>et al.</i>	<i>nrfA-2R</i>	CCGGCACTTTCGAGCCC		
703	(2007)	<i>nrfA-2 TM*</i>	TTGACCGTCGGCA		
704	<i>nirS-e</i>	<i>nirS-ef-F</i>	CACCCGGAGTTCATCGTC	172	60
705	Smith <i>et al.</i>	<i>nirS-efR</i>	ACCTTGTTGGACTGGTGGG		

706	(2007)	<i>nirS</i> -ef	TM*	TGCTGGTCAACTA		
707		<i>nirS</i> -m	<i>nirS</i> -m-F	GGAAACCTGTTCGTCAAGAC	162	60)
708	Smith <i>et al.</i>	<i>nirS</i> -mR		CSGARTCCTTGGCGACGT		
709	(2007)	<i>nirS</i> -m	TM	TCTGGGCCGACGCGCCGATGAAC		
710		<i>nirS</i> -n	<i>nirS</i> -n-F	AAGGAAGTCTGGATYTC	140	55
711	Smith <i>et al.</i>	<i>nirS</i> -nR		CGTTGAACTTRCCGGT		
712	(2007)	<i>nirS</i> -n	TM*	ATCCGAAGATSA		

713 Legend: *TM *TaqMan* Minor Groove Binding; TM, *TaqMan*

714
715

716 **Table 2:** Quantitative and reverse transcriptase quantitative -PCR standard curve descriptors

717

718	Phylotype	Template	r^2	y-intercept	<i>E</i> (%)	Ct-cutoff
719	16S rRNA	DNA	0.998	35.1	92.6	28.9
720	<i>narG</i> -1	DNA	0.998	41.1	77.6	29.9
721	<i>narG</i> -2	DNA	0.998	43.4	85.4	ND
722	<i>napA</i> -1	DNA	0.994	44.7	95.5	32.3
723	<i>napA</i> -2	DNA	0.999	42.2	86.9	31.3
724	<i>napA</i> -3	DNA	0.997	41.9	89.9	34.1
725	<i>nirS</i> -ef	DNA	0.998	35.0	86.0	35.9
726	<i>nirS</i> -m	DNA	0.996	41.1	86.0	ND
727	<i>nirS</i> -n	DNA	0.998	42.8	82.1	ND
728	<i>nrfA</i> -2	DNA	0.997	39.9	96.0	28.5
729	<i>narG</i> -2	cDNA	0.999	43.3	83.0	ND
730	<i>nirS</i> -ef	cDNA	0.998	43.0	85.0	ND

731

732 Legend: *E* = amplification efficiency, ND= no template control not detected

733

734

735

736

737

738

739

740 **Table 3:** Spearman's rank correlation co-efficient between rate process measurements and
741 functional gene abundances

742	Rate Process	gene	<i>r</i>	<i>P</i>	n
743	Denitrification	<i>nirS-ef</i>	0.422	0.081	18
744		<i>nirS-n</i>	0.562	0.015*	18
745		<i>nirS-m</i>	0.608	0.007*	18
746	DNRA	<i>nrfA</i>	0.485	0.056	18

747 * $P < 0.05$

Figure 1.TIFF

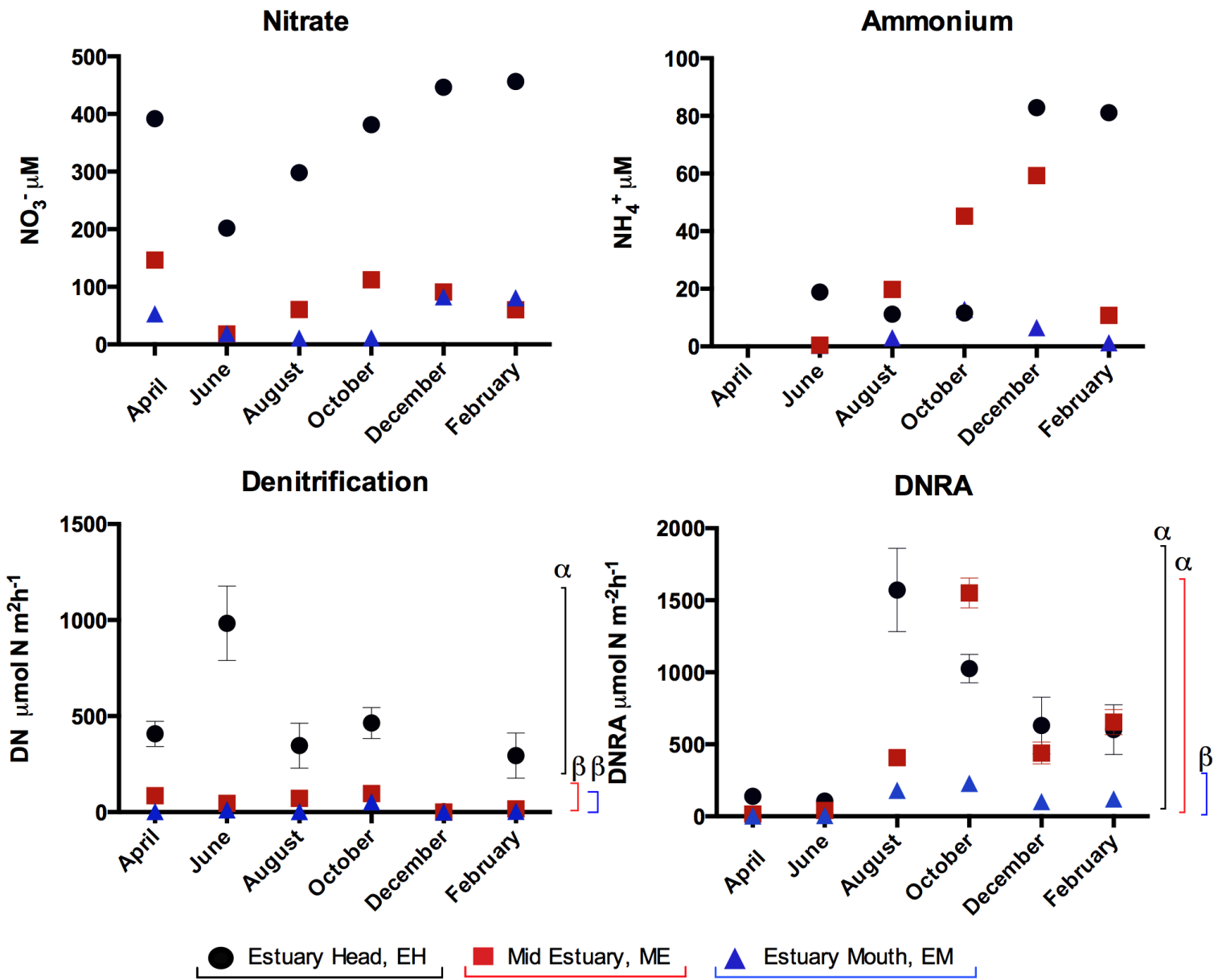


Figure 2.JPEG

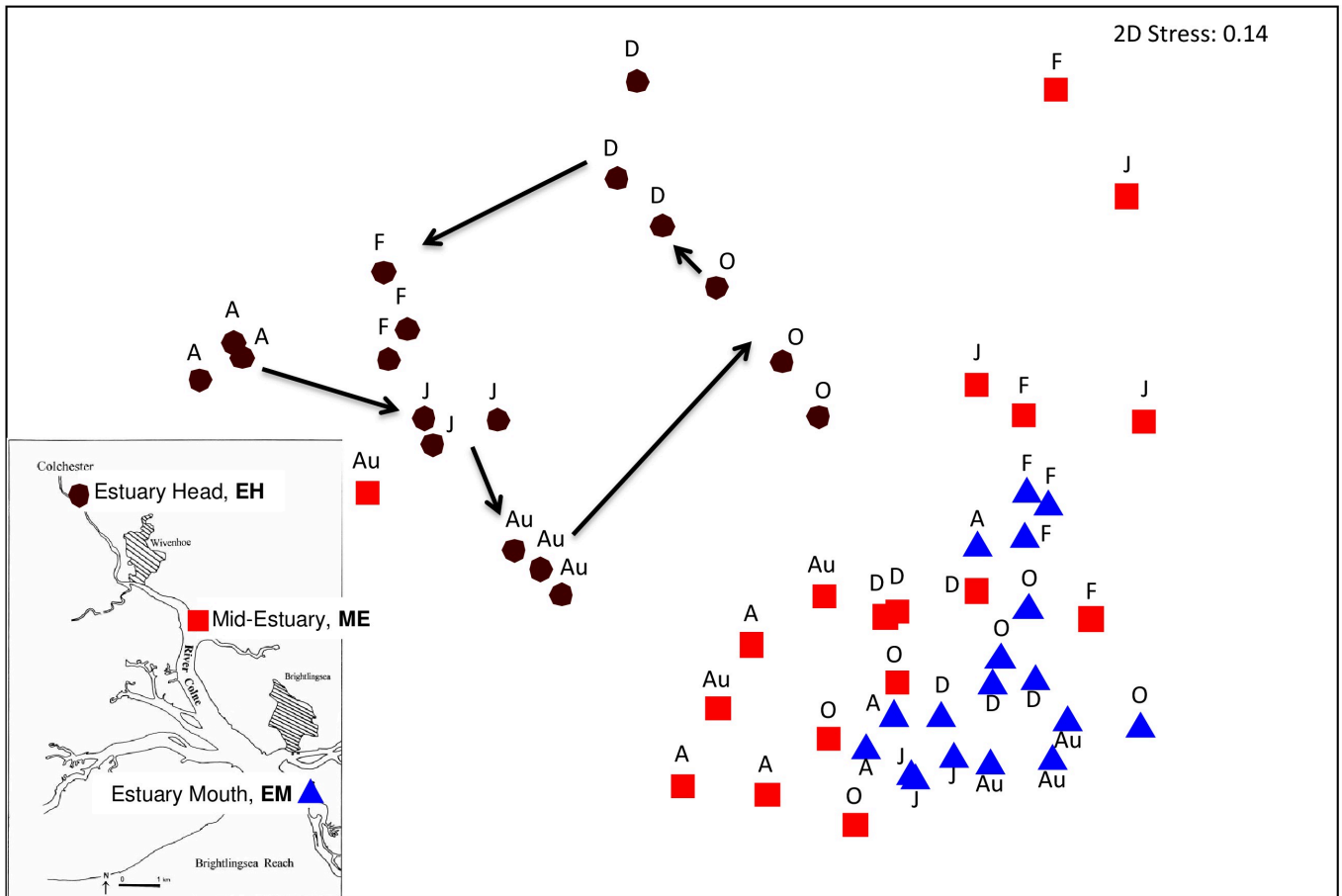


Figure 3.TIFF

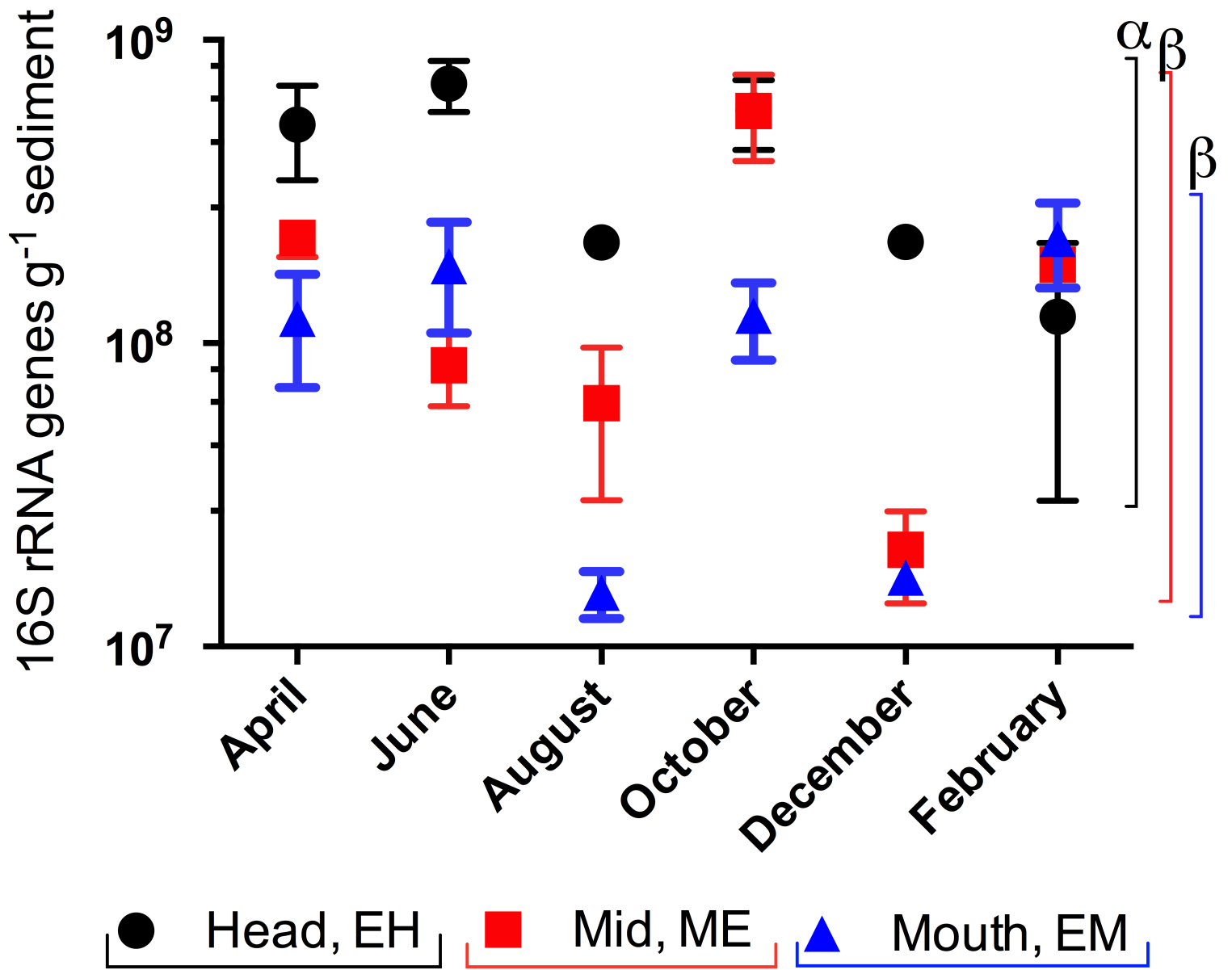


Figure 4.JPEG

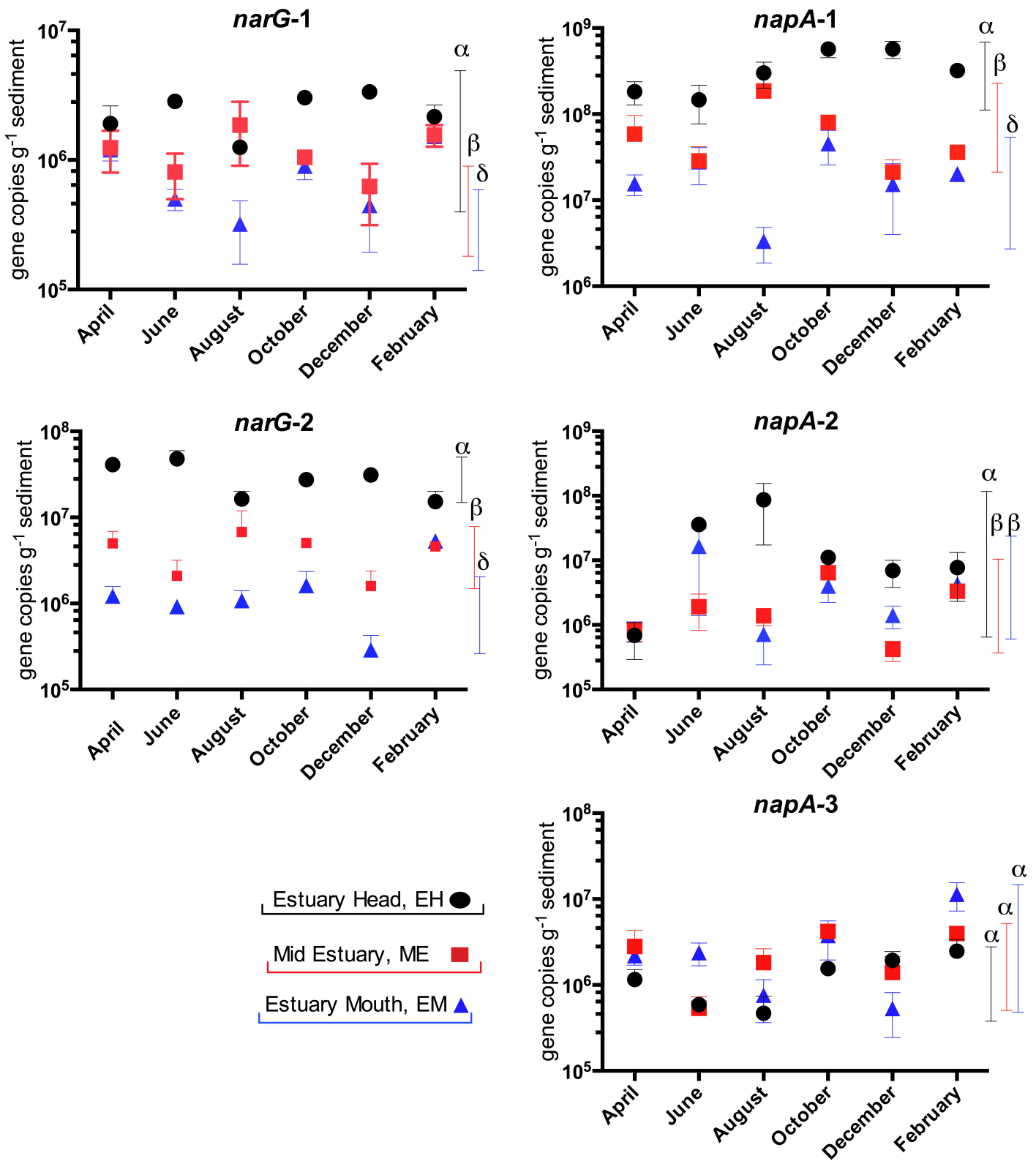


Figure 5.TIFF

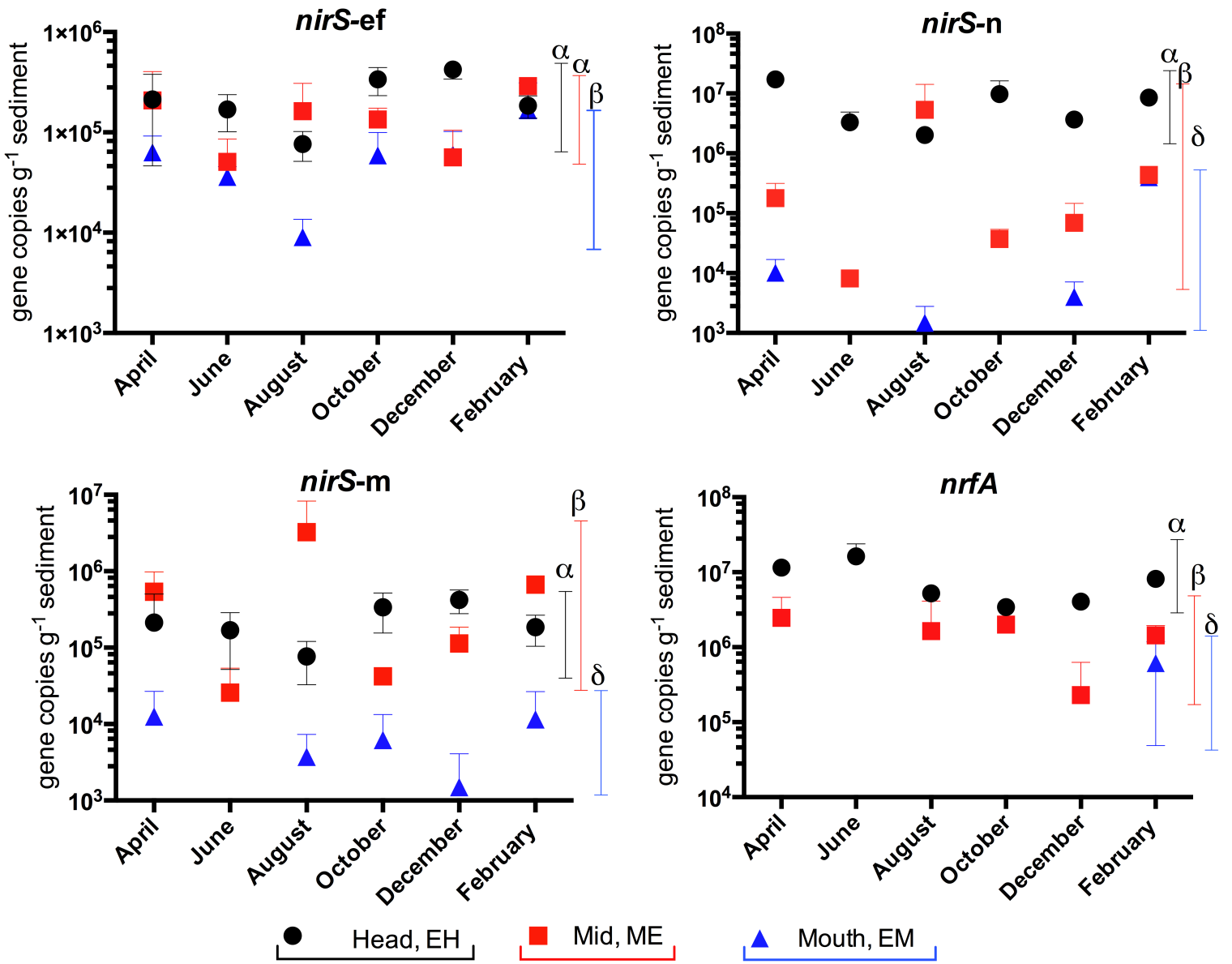


Figure 6.TIFF

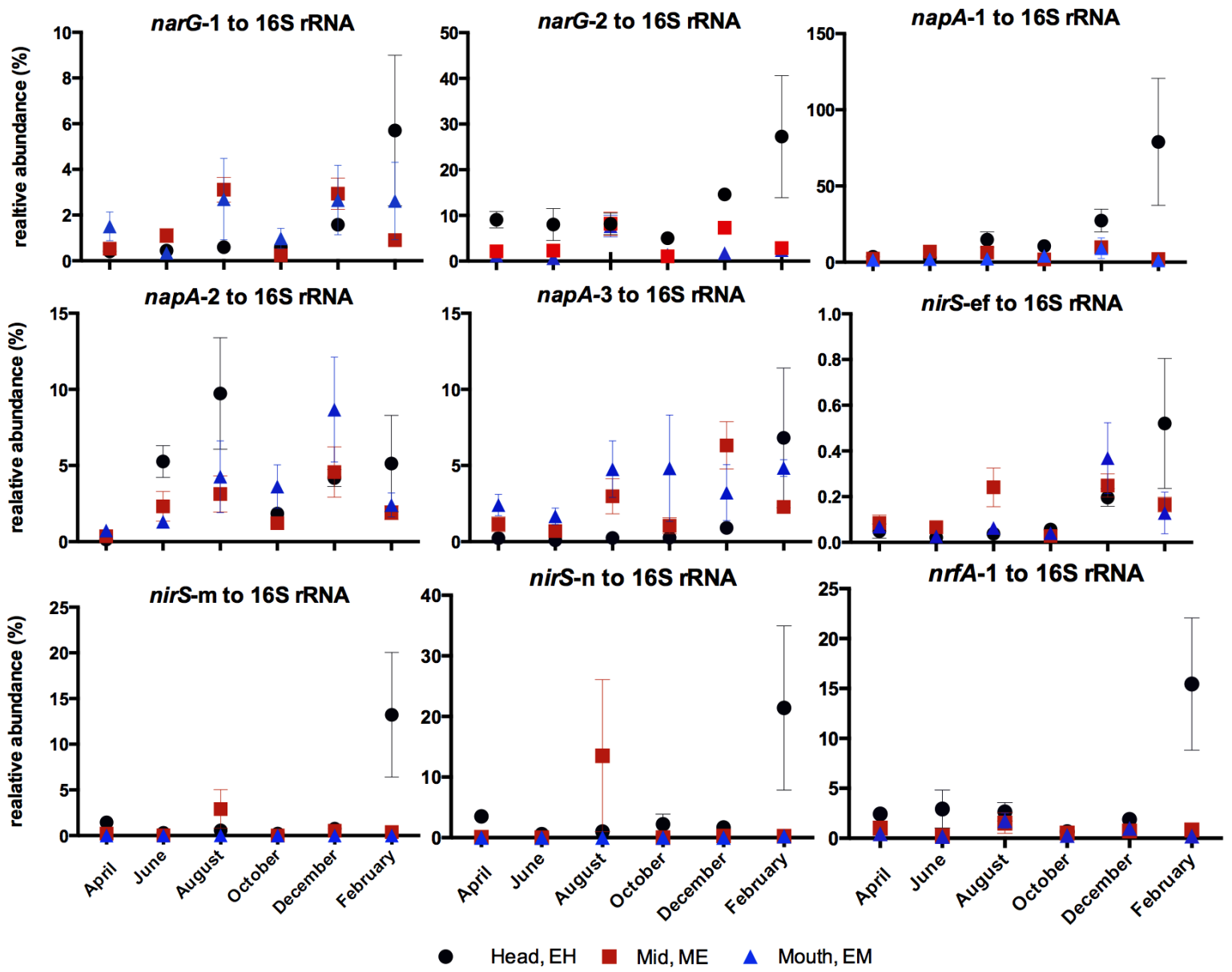
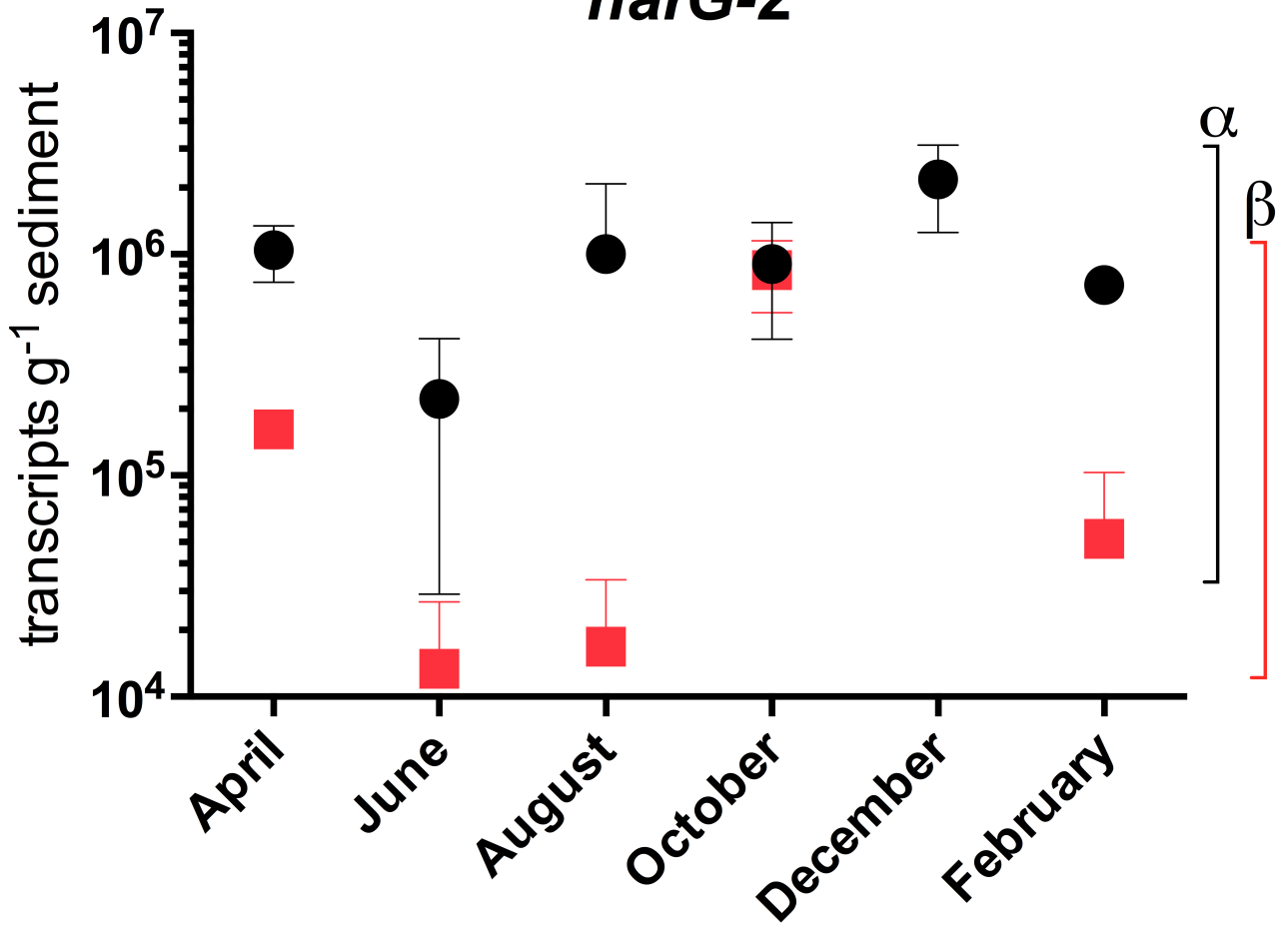


Figure 7.TIFF

narG-2



nirS-ef

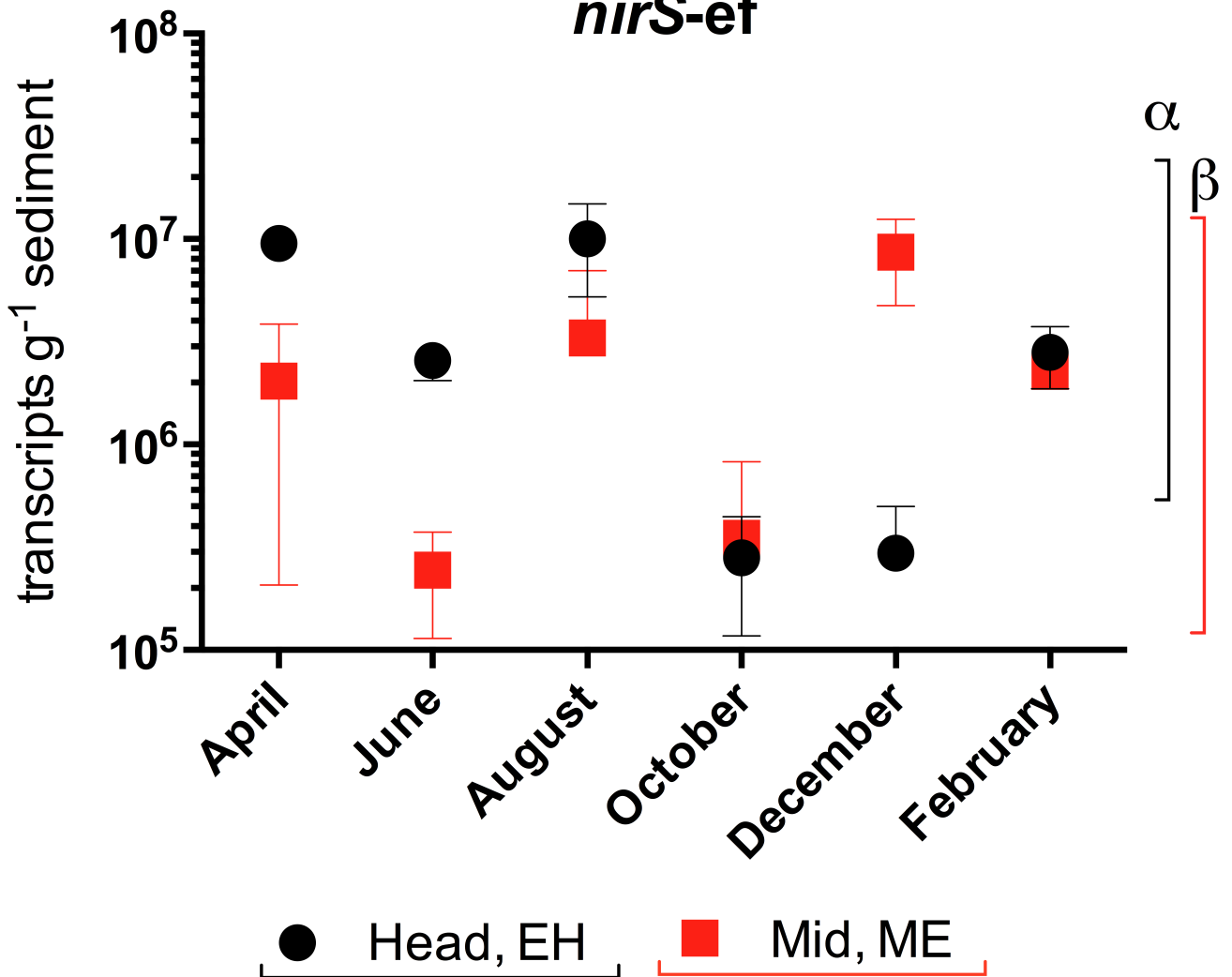


Figure 8.JPEG

